

THE PENNSYLVANIA STATE UNIVERSITY
SCHREYER HONORS COLLEGE

DEPARTMENT OF BIOMEDICAL ENGINEERING

Assessing the Degradation of Novel Neural Prostheses Using Real Time Shear Wave
Elastography, Ultrasound, and Photoacoustic Imaging Tools

HANNA DROZYNSKI
SPRING 2022

A thesis
submitted in partial fulfillment
of the requirements
for a baccalaureate degree in Biomedical Engineering
with honors in Biomedical Engineering

Reviewed and approved* by the following:

Sri-Rajasekhar Kothapalli
Assistant Professor of Biomedical Engineering
Thesis Supervisor

Meghan Vidt
Assistant Professor of Biomedical Engineering
Honors Adviser

* Electronic approvals are on file.

ABSTRACT

Neural prostheses are crucial for patients with peripheral nerve damage in regaining their motor and sensory functions. Materials used in such prostheses must be biologically compatible, anti-inflammatory, have a slow degradation time, and be mechanically strong. This work studies the degradation of biodegradable photoluminescent polymers + aniline tetramer (BPLP+AT) and poly(1,8-octanediol citrate) + folic acid (POC-FA) as biomaterials that bridge gaps in peripheral nerves. The materials are imaged at different levels of degradation using a novel multimodal imaging probe that shows ultrasound, photoacoustic, and shear wave elastography images. Combined, these images show that an increase in the percentage of AT in BPLP-AT leads to a decrease in the material's shear modulus. On the contrary, the increase in the percentage of FA in POC-FA leads to an increase in the material's shear modulus.

Additionally, it was found that an increase in the percent of AT in BPLP decreases the light absorbing properties while an increase in the percent of FA in POC increases the light absorbing properties. Moreover, the longer the material degrades, the less light absorbing it is.

TABLE OF CONTENTS

LIST OF FIGURES	iii
ACKNOWLEDGEMENTS	v
Chapter 1 Neural Prostheses	1
Anatomy of a Neuron.....	1
Diagnosis and Treatment.....	2
Autologous and Allografts	3
Collagen Based Nerve Implants.....	4
Poly (DL-lactide- ϵ -caprolactone).....	4
BPLP-AT and POC-FA.....	5
Chapter 2 Medical Imaging	7
Ultrasound.....	8
Photoacoustic	9
Shear Wave Elastography	10
Chapter 3 Methods	11
BPLP-AT and POC-FA Fabrication	11
Phantom Fabrication	12
Imaging Phantoms.....	15
Chapter 4 Results and Discussion.....	18
SWE Images.....	18
USPA Images.....	26
Chapter 5 Conclusion.....	30

LIST OF FIGURES

Figure 1: Peripheral Neurons	2
Figure 2: Ultrasound Setup [27]	9
Figure 3: Shear Wave Elastography Diagram.....	10
Figure 4: BPLP-AT 5% Degraded at 1, 2, 4, 8, and 12 Hours.....	13
Figure 5: Five Phantoms Fabricated	14
Figure 6: USPA Imaging Setup	15
Figure 7: SWE Imaging Setup	16
Figure 8: Shear Wave Focus for (a.) BPLP-AT Samples, (b.) POC-FA Samples and (c.) the Continually Degraded BPLP-AT 5% Samples	16
Figure 9: SWE Nondegraded BPLP-AT 5%, 10% Right Side Filtered.....	18
Figure 10: SWE Nondegraded BPLP-AT 5%, 10% Left Side Filtered	19
Figure 11: SWE Nondegraded POC-FA 5%, 10% Right Side Filtered.....	19
Figure 12: SWE Nondegraded POC-FA 5%, 10% Left Side Filtered	20
Figure 13: SWE 1 Hour Degraded BPLP-AT 5%, 10% Right Side Filtered.....	20
Figure 14: SWE 1 Hour Degraded BPLP-AT 5%, 10% Left Side Filtered	21
Figure 15: SWE 1 Hour Degraded POC-FA 5%, 10% Right Side Filtered.....	21
Figure 16: SWE 1 Hour Degraded POC-FA 5%, 10% Left Side Filtered	21
Figure 17: SWE 2 Hours Degraded BPLP-AT 5%, 10% Right Side Filtered	22
Figure 18: SWE 2 Hours Degraded BPLP-AT 5%, 10% Left Side Filtered	22
Figure 19: SWE 2 Hours Degraded POC-FA 5%, 10% Right Side Filtered	23
Figure 20: SWE 2 Hours Degraded POC-FA 5%, 10% Left Side Filtered	23
Figure 21: SWE 4 Hours Degraded BPLP-AT 5%, 10% Right Side Filtered	23
Figure 22: SWE 4 Hours Degraded BPLP-AT 5%, 10% Left Side Filtered	24
Figure 23: SWE 4 Hours Degraded POC-FA 5%, 10% Right Side Filtered	24
Figure 24: SWE 4 Hours Degraded POC-FA 5%, 10% Left Side Filtered	24

Figure 25: SWE 1, 2, 4, 8, 12 Hours Degraded BPLP-AT 5% Right Side Filtered.....	25
Figure 26: SWE 1, 2, 4, 8, 12 Hours Degraded BPLP-AT 5% Left Side Filtered.....	25
Figure 27: BPLP-AT 5%, 10% and POC-FA 5%, 10% Phantoms - All Levels of Degradation and BPLP-AT 5% Continual Degradation Phantom.....	26
Figure 28: USPA Nondegraded BPLP-AT 5%, 10% and POC-FA 5%, 10%	27
Figure 29: USPA 1 Hour Degraded BPLP-AT 5%, 10% and POC-FA 5%, 10%	28
Figure 30: USPA 2 Hours Degraded BPLP-AT 5%, 10% and POC-FA 5%, 10%	28
Figure 31: USPA 4 Hours Degraded BPLP-AT 5%, 10% and POC-FA 5%, 10%	29
Figure 32: USPA 1, 2, 4, 8, 12 Hours Degraded BPLP-AT 5%	29

ACKNOWLEDGEMENTS

My utmost thanks and appreciation to

Dr. Sri-Rajasekhar Kothapalli
for mentoring me and taking time to continually meeting with me
and teaching me the ropes of how to be a good researcher

Dr. Meghan Vidt
for always answering my questions
and assisting me with any logistical problems that arose

Dr. Jian Yang
for providing interdisciplinary materials and information from his lab

Abigail Haworth
for teaching me how to use the laboratory equipment with proper techniques
and for supervising my experiments

Dingbowen Wang
for being a great point of contact between labs
and for providing me with all the biomaterials necessary for this study

Chapter 1

Neural Prostheses

The nervous system is separated into two parts, the central nervous system (CNS) and the peripheral nervous system (PNS). The CNS consists of the nerves in the brain and spinal cord while the PNS is a network made up of all the remaining motor, sensory and autonomic nerves in the body. The PNS is an anatomical link between the environment and the CNS, it is responsible for detecting changes in one's surroundings and relaying the information to the CNS. [1]

Peripheral nerve damage can occur in many ways. The most common way to sustain a peripheral nerve injury is from an injury in which the nerve is stretched, torn, or crushed. In addition to the injury related neuropathies, there are hereditary neuropathies, a group of disorders that are inherited genetically, that can directly affect the peripheral nervous system such as lupus, carpal tunnel syndrome and rheumatoid arthritis. Likewise, there are acquired factors such as diabetes, thyroid disease or alcohol abuse that can lead to neuropathies. [2-3]

Anatomy of a Neuron

There are four main components in a neuron: the dendrites, the cell body, the axon, and the myelin sheath. The dendrites are branched extensions of the neuron that detect electrical signals from surrounding neurons. These signals are sent to the cell body of the neuron where they are processed by the nucleus. Next, the cell body sends the signals along the axon to be received by other neurons. [4] The myelin sheath is a protective layer of proteins and fatty substances that coats the axon to allow it to transfer signals efficiently. [5] In a damaged

peripheral nerve, the axon is partially or completely severed, resulting in loss of communication between the two parts of the nerve. Figure 1 shows graphics of a healthy and damaged peripheral nerve.

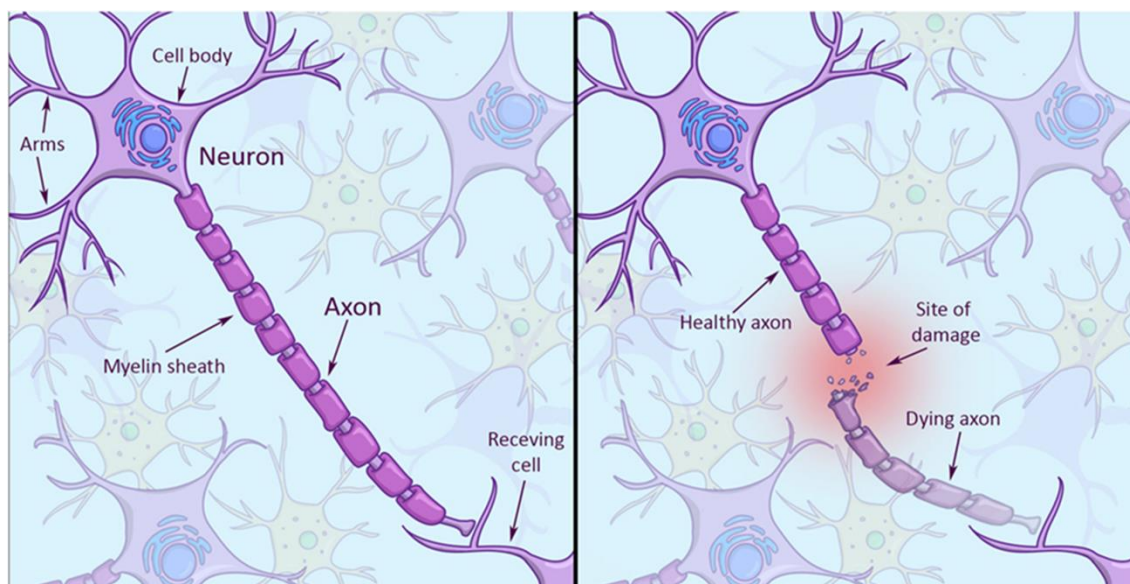


Figure 1: Peripheral Neurons

Healthy (left) and damaged (right) peripheral neurons [6]

Diagnosis and Treatment

Injured peripheral nerves can cause numbness, tingling, a burning sensation, or sharp pains in the affected area. To diagnose the nerve damage, a few different tests can be run, including a nerve conduction study, an electromyography (EMG), a magnetic resonance image (MRI) or a high-resolution ultrasound.

A nerve conduction study measures the electrical impulses in one end of the nerve resulting from a slight current introduced at the other end of the nerve. An EMG studies the electrical activity in your muscles when they are in use and when they are at rest. Finally, MRIs

and high-resolution ultrasounds are methods of producing detailed images of the body which can be analyzed and scanned for nerve root compression. [7]

After a peripheral nerve damage diagnosis is made, a treatment plan is formed. Current clinical treatments include rest, a splint or brace, physical therapy, nonsteroidal anti-inflammatory drugs (NSAIDs) or even surgery to take pressure off the injured nerve. [7] There is research being done that studies the use of various biomaterials and their effectiveness as a neural prosthesis to bridge the gap in neuron deficits. These biomaterials include but are not limited to autologous tissue, human nerve allografts, collagen, and poly (DL-lactide- ϵ -caprolactone).

Autologous Nerve Grafts and Allografts

An autologous nerve graft is one that uses a nerve from a different location in the patient's body as the graft for the site of interest. Autologous nerve grafts are very popular because they often have a high rate of success and have high rates of returning function to the affected areas. [8] Because the nerve graft is sourced directly from the patient, there is a low risk of the body rejecting the graft. Despite the many advantages to autologous grafts, there are significant downfalls to this method of nerve grafting. Firstly, this method requires a surgery at the site of the nerve source. Every surgery has its risk of complications such as infection. Since the portion of nerve used for the graft is from the patient's own body, there is risk of losing neural function in the location in which the replacement nerve was taken from. Additionally, if the initial sourcing surgery fails, the patient will now be left with two sites of peripheral nerve damage.

A solution that eliminates the autologous sourcing surgical concerns is a human nerve allograft. A nerve allograft is a nerve graft from a donor of the same species as the recipient but not genetically identical. AxoGen Avance is the only FDA approved human nerve allograft. [9-10] Brooks et al. studied the efficacy of the Avance allograft compared to autologous nerve grafts. They found the two nerve grafts were comparable in nerve injuries between 5-50 mm. However, with larger peripheral nerve injuries, the autologous grafts were superior. [11] Because of the downfalls of autologous nerve grafting, and the limitations of human nerve allografts, there has been significant research about novel biomaterials to be used as neural prostheses.

Collagen Based Nerve Implants

Collagen is a fundamental protein found in the body. It makes up skin, bone, and connective tissues. [12] Collagen is a viable biomaterial to encourage tissue regeneration, making it a good choice for a neural prostheses scaffolding. [13] Masand et al. evaluated the use of collagen hydrogels functionalized with polysialic acid (PSA) and human natural killer-1 (HNK-1) carbohydrate. Both glycans have been independently shown to encourage nerve regeneration and axonal targeting. They found that PSA-coupled collagen improved axon number, whereas HNK-1-coupled collagen improved motoneuron targeting and myelination of axons. [14]

Poly (DL-lactide- ϵ -caprolactone)

Dunnen et al. demonstrate that biodegradable nerve guides constructed of Poly (DL-lactide- ϵ -caprolactone) perform better than autologous nerve grafts and that these nerve guides

do not have the disadvantages of the silicone nerve conduits since they gradually disappear after serving their function [15].

Neurolac is an FDA approved Poly (DL-lactide- ϵ -caprolactone) nerve conduit. Because it is resorptive and semi-permeable, Neurolac has the same advantages as other synthetic guides for nerve regeneration. Similarly, Neurolac is only able to be used for nerve defects less than 2 cm and is very expensive, giving it the same disadvantages as other synthetic guides for nerve regeneration. Unlike other guides, it presents the advantage of its transparency but also the disadvantage of its mechanical hardness. Chiriac et al. studied the use of a Neurolac nerve conduit on 28 peripheral nerve injuries and had results that did not favor the use of Neurolac for repairing hand nerve defects. [16]

BPLP-AT and POC-FA

Citric acid (CA) is an important intermediate in the citric acid cycle and occurs in the metabolism of all aerobic organisms. [17] Because of its high reactivity due to the presence of one hydroxyl and three carboxyl groups, CA has become one of the most frequently used molecules for the synthesis of biocompatible fluorescent materials.

Yang and co-workers from Shan et al. [18] discovered a set of biodegradable photoluminescent polymers (BPLPs) were developed with fluorophores formed by reacting CA and amine-containing molecules including amino acids. BPLPs demonstrated in vitro cytocompatibility, desired mechanical properties, excellent processability for micro and nanofabrication, as well as strong fluorescence.

Poly(1,8-octanediol citrate) (POC) is a biodegradable elastomer that has good cytocompatibility and similar mechanical properties to soft tissues. [19] Folic acid (FA), is a

vitamin B derivative that is known to have high versatility in its uses but has increasing popularity due to its effectiveness of enhancing tissue regeneration. [20]

Together they make a biomaterial, POC-FA, that combines the good qualities of both materials. Li et al. studied the efficacy of the POC-FA as a film that could be used as a scaffold material for neural tissue engineering. [21] They found that the film improves hydrophilicity and promotes cell activity for PC12 cell attachment as well as cells with more neurite extension.

Although Li et al. has shown significant proof that POC-FA is a suitable scaffold material for neural tissue. There have been no studies on how this material breaks down over time. Or how they reach to torsion and bending. These are important concepts if the materials are expected to keep its integrity for a long time in the body. In this thesis, I close this gap in research by studying the degradation and shear modulus of the biomaterials BPLP-AT and POC-FA.

Chapter 2

Medical Imaging

Medical imaging has high importance in the detection and diagnosing of various diseases. There are different qualities of medical imaging that can make it more useful in different clinical scenarios. One quality is the device's image processing time. Some devices have real time image processing while others need post image editing. An ultrasound of a pregnant woman is an example of medical imaging that does not need post imaging processing. An obvious advantage to real time image processing is that a clinician does not have to wait to view the images and risk the patient's situation worsening. However, some imaging devices, such as magnetic resonance imaging (MRI) require post imaging processing to make the image readable and meaningful to a radiology technician.

In addition to image processing time, qualities of medical imaging devices that effect their favorability are invasiveness, the use of dyes or agents, imaging depth, reliance on user, radiation exposure, portability, cost, and perhaps most importantly, what tissues the modality can decipher between.

Recent studies involving the assessment of the function of biomaterials as a neural conduit use imaging methods such as MRI and computer tomography (CT) [22-25] This is problematic because neither of these modalities are portable and they require a foreign dye to be injected into the subject. Additionally, CT introduces radiation to the subject. To better assess the function of neural conduits in real time, a multimodal, handheld imaging tool should be used. The proposed device was first implemented by Dr. Sri-Rajasekhar Kothappali's laboratory on The Pennsylvania State University's campus. This device simultaneously takes ultrasound, photoacoustic and shear wave elastography images, producing a comprehensive image of the

target. Because of its' portability, radiation free and real time qualities, this device will allow for image guided surgeries as well.

Ultrasound

Ultrasound imaging (US) is a very safe, widely used imaging technique often used to study soft tissue. Shown in Figure 2, ultrasound devices are comprised of a probe with a transducer wired to a computer and a monitor for image viewing. The first step in the process of generating an ultrasound image is to couple the transducer to the skin of the subject with a gel to create a seamless transition between the two. Once coupled, the transducer sends high frequency sound waves into the subject. These sound waves have no trouble passing through soft tissue. However, when they reach a boundary interface that has fluid, such as an area that layers soft tissues from two different organs, some of the soundwaves echo back toward the transducer. The transducer sends these signals to the computer which can interpret the reflected soundwaves and return an image of the internal structures of the subject being studied. [26] Ultrasound imaging is portable, low-cost, and very safe; however, it is ineffective in providing molecular contrast.

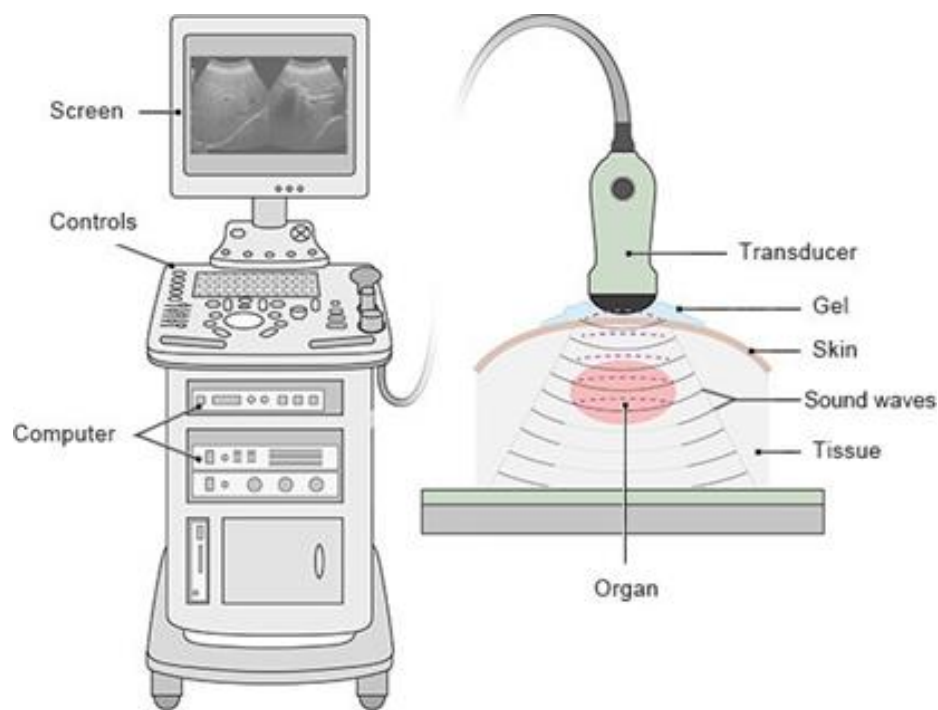


Figure 2: Ultrasound Setup [27]

Photoacoustic

Photoacoustic imaging (PA) is a hybrid imaging modality that combines the qualities of optical imaging and ultrasound imaging. Contrary to ultrasound imaging as an independent imaging modality, photoacoustic imaging does a fantastic job differentiating between structure specific molecules. [28-29] In photoacoustic imaging, pulses of light from a laser are sent into the subject. Chromophores such as water, lipids, and hemoglobin in red blood cells absorb the light which causes temperature increases and localized thermoelastic expansion. Pressure and sound waves radiate from the structures that have undergone thermoelastic expansion. A high frequency transducer recognizes these signals and sends them to a computer where they are analyzed. The computer generates a real time, molecule specific image. [30-31] Photoacoustic

imaging is unique in the way that it can differentiate between structures based on the tissues' optical absorption, providing greater specificity than ultrasound imaging.

Shear Wave Elastography

Shear wave elastography (SWE) is a relatively new technique of medical imaging. It is an imaging technique that is used to help evaluate soft tissue elasticity. SWE uses an acoustic radiation force pulse sequence to generate shear waves, which propagate perpendicular to the ultrasound beam, causing transient displacements. The distribution of shear-wave velocities at each pixel is directly related to the shear modulus, an absolute measure of the tissue's elastic properties. [32] Figure 3 shows the progression of how SWE functions. In the first step, the shear waves are generated. Next, fast plane wave excitation is used to track displacement and velocity as shear waves propagate. Finally, the shear modulus can be calculated. [32]

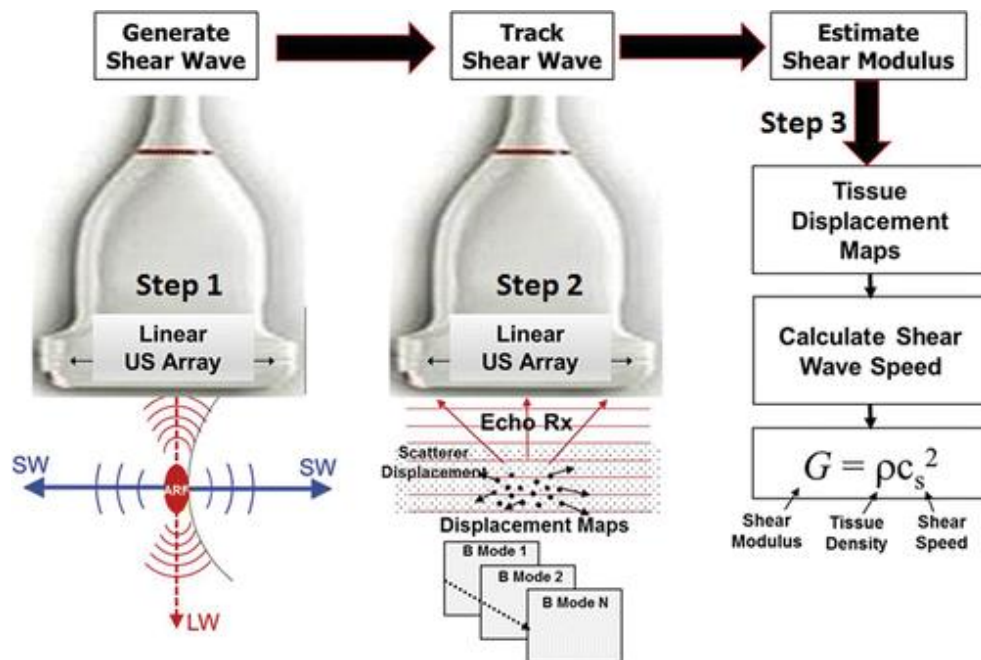


Figure 3: Shear Wave Elastography Diagram

Chapter 3

Methods

To assess the degradation of BPLP-AT and POC-FA, an experiment was conducted. First, five agarose-silica phantoms were fabricated. The samples were organized in the phantoms based on their weight percentages and degradation times. The phantoms were imaged using the linear multimodal probe for US and PA. SWE imaging was done separately.

BPLP-AT and POC-FA Fabrication

The BPLP-AT prepolymer was synthesized via a one-pot polycondensation reaction. Citric acid (CA), 1,8-octanediol (OD), L-cysteine, and aniline tetramer (AT) at molar ratios of 1: 1.2: 0.2: 0.05/0.10 were added to a round-bottom flask, and the reaction was carried out at 110 °C under a nitrogen atmosphere for five hours.

The POC-FA prepolymer was also synthesized via a one-pot polycondensation reaction. Citric acid (CA), 1,8-octanediol (OD), and folic acid (FA) at molar ratios of 1: 1: 0.05/0.10 were used. CA and OD were first added to a round-bottom flask and were melted at 160 °C. The FA was added and the reaction temperature was reduced to 140 °. The reaction was carried out under a nitrogen atmosphere until the stirring speed reduced to 60 rpm.

The prepolymers were dissolved in 1,4-dioxane and purified by precipitating the solution into distilled water. Finally, the prepolymers were lyophilized for 24 hours and stored in a drying chamber until further use. According to the theoretical molar ratios of FA and AT to CA, which were set as 5% and 10%, the samples are now referred to as POC-FA 5%, POC-FA 10%, BPLP-AT 5% and BPLP-AT 10% respectively.

To prepare POC-FA and BPLP-AT films, respective pre-polymers in dioxane were cast onto Teflon molds, followed by evaporation and thermal crosslinking at 80°C (POC-FA) or 100°C (BPLP-AT) for 3 days. In this thermal process, un-reacted -COOH and -OH groups of pre-polymers are cross-linked into an elastomeric network.

The BPLP-AT and POC-FA films were cut into discs, 5mm in diameter. Some of the discs were set aside for nondegraded imaging while others were degraded. The films being degraded were each put into an individual 15mL centrifuge tube and degraded in 10mL of a 0.2M NaOH solution in a shaker set at 100rpm for one, two, four, eight and twelve hours. This process occurred at 37 °C.

Phantom Fabrication

Using the BPLP-AT and POC-FA samples, phantoms were fabricated for imaging. Five phantoms were made, organized by AT and FA weight percentage as well as length of degradation. The phantoms made, imitate the properties of human tissue.

To prepare the phantoms, first a 150 mL solution of distilled water, agarose and fumed silica was made with a 1: 0.015: 0.01 ratio by weight respectively. This solution was microwaved in 1-minute increments with light swirling of the flask every minute until the agarose and fumed silica were dissolved. Caution was taken to swirl the flask gently as to make as few bubbles as possible. The solution was taken into the cold room which was set at 4 °C. The cold room accelerated the solidification of the agarose and silica solution. While in the cold room, the solution was gently but continuously swirled. Just before the solution solidified it was poured from the flask into a 75mm x 75mm x 75mm plastic box, leaving 17.5mm of space at the top,

which was measured prior to pouring the solution. It was important to pour the solution before it solidified so the surface remained smooth and without lumps, but it was just as important to not pour the solution too early or the silica particles sank to the bottom before solidifying.

Once the bottom layer of agarose and silica solidified, the BPLP-AT and POC-FA samples were added to the phantom. Small discs of the samples were cut out. The diameters of the discs all started at approximately 5 mm. As the discs degraded their given amounts, they shrunk. These samples were placed on the surface of the phantom with approximately 3mm of space in between samples. Figure 4 shows the setup of the bottom layer of a representative phantom.

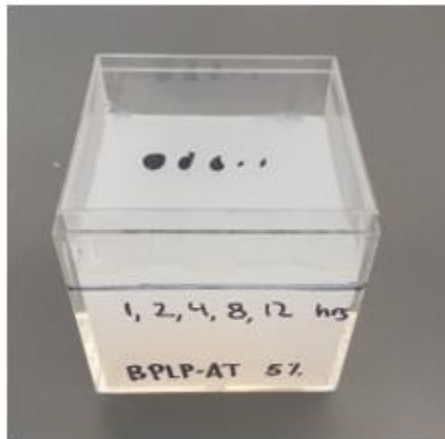


Figure 4: BPLP-AT 5% Degraded at 1, 2, 4, 8, and 12 Hours

After these steps are done, another batch of the distilled water, agarose and silica solution was made. Like before, the solution was taken into the cold room for faster solidification. Once the solution was almost cooled enough to solidify, a few drops were pipetted over the samples. This helped mount them down so, when the rest of the solution was poured over them, they did not float or move in any way. When the solution was cool, the plastic box was filled to the top with the solution. The same process was repeated for the other four phantoms.

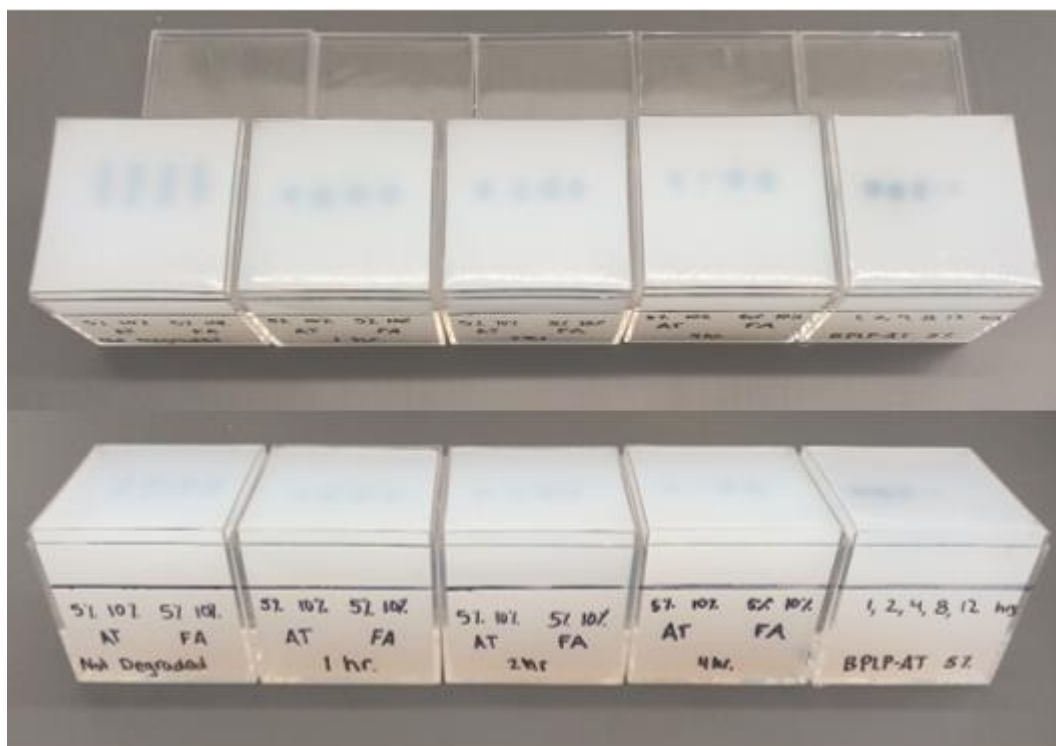


Figure 5: Five Phantoms Fabricated

There were five total phantoms fabricated. Figure 5 shows the different phantoms fabricated. The four on the left each have one sample of BPLP-AT 5%, BPLP-AT 10%, POC-FA 5%, and POC-FA 10%. The first phantom has these four materials with no degradation. The second phantom is degraded for one hour, the third phantom for two hours and the fourth phantom for four hours. The last phantom contains five samples of BPLP-AT 5% with degradations of one, two, four, eight, and twelve hours. This combination of phantoms was made so the two materials at similar degradation times could be compared as well as the continual degradation of the same material, BPLP-AT 5%. BPLP-AT 5% was the only material chosen for the continual degradation study because the other materials were either completely degraded or there was no supply.

Imaging Phantoms

After the samples were prepared, it was time to image them. First, the phantoms were imaged using the ultrasound and photoacoustic (USPA) linear probe. Figure 6 shows the laboratory set up of the phantom, probe and biomaterials. The probe was connected to a Verasonics Vantage system which interpreted all of the signals read by the transducer. The time gain compensation (TGC) was set for all layers of the phantom and kept consistent across phantoms. This is especially important for the PA images since the contrast in the image has a direct correlation to the material's light absorption properties.

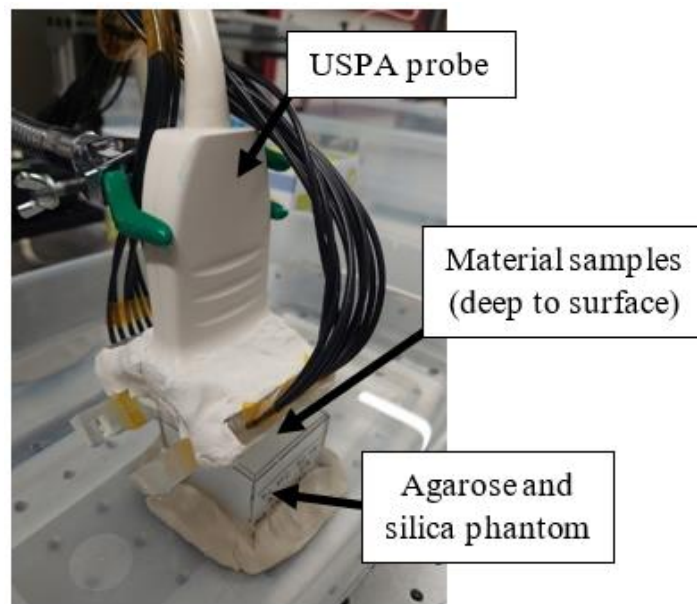


Figure 6: USPA Imaging Setup

After all the phantoms were imaged using the USPA linear probe, SWE images were taken. Similar to the USPA imaging, the SWE linear probe was connected to the Verasonics Vantage system. Figure 7 shows the laboratory setup of the phantom, probe and biomaterials.

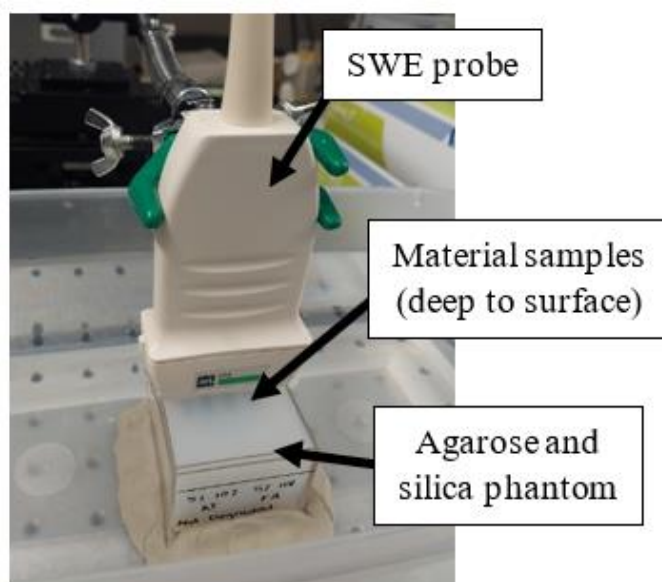


Figure 7: SWE Imaging Setup

During SWE imaging, a consistent voltage of 30 volts was used across all images. A focus point had to be chosen for where the transducer will propagate the shear waves from. After some experimental trials, it was found the best SWE images are produced when the focus is set below the samples. Figure 8a shows where the focus was set for imaging the BPLP-AT samples. Figure 8b shows where the focus was set for imaging the POC-FA samples. Finally, Figure 8c shows where the focus was for the continual degradation of BPLP-AT 5% samples.

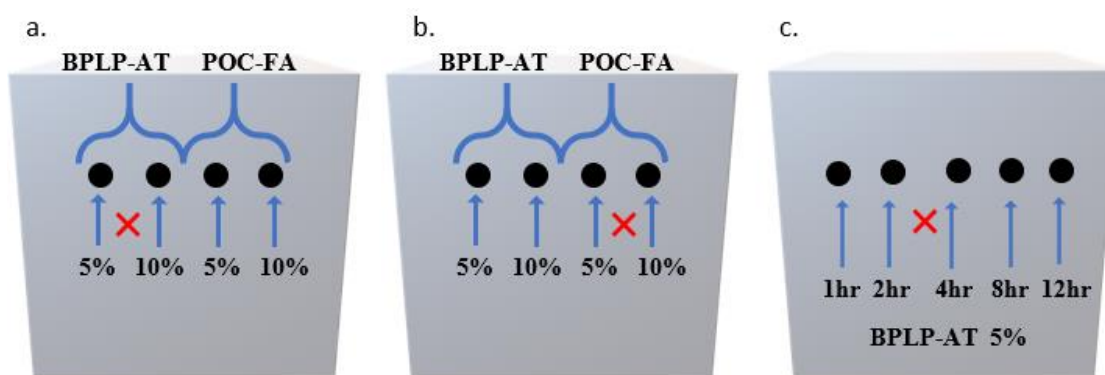


Figure 8: Shear Wave Focus for (a.) BPLP-AT Samples, (b.) POC-FA Samples and (c.) the Continually Degraded BPLP-AT 5% Samples

Each SWE image has to be filtered on either the right or left side. This means that, for example, if the BPLP-AT material was being looked at and the right side was being filtered, the BPLP-AT 5% sample is the one in focus. If the left side was being filtered, the BPLP-AT 10% sample is the one in focus. Because of this, comparisons between like materials of different percentages can only be made with a right-filtered and a left-filtered image of the same focus.

Chapter 4

Results and Discussion

The following images were produced using SWE and USPA imaging techniques described in Chapter 3. Each shear wave elastography figures has three sub images. These images are the US reference, the absolute velocity of the shear wave being propagated and the material's shear modulus. Because some of the absolute velocity and shear modulus images have lots of noise, the US reference is helpful in depicting where the biomaterial targets are located in the phantom.

SWE Images

Figures 9 and 10 show the US reference, the absolute velocity of the shear wave propagated, and the shear modulus of the material of the nondegraded BPLP-AT 5% sample and BPLP-AT 10% sample respectively. It is seen by comparing the left side of the shear modulus contour plot in Figure 9 (BPLP-AT 5%) to the right side of the shear modulus contour plot in Figure 10 (BPLP-AT 10%), that an increase in the percent of AT added to BPLP leads to a decrease in the material's shear modulus. This is seen by a less intense marking in the locations of each material as seen in the respective US reference images.

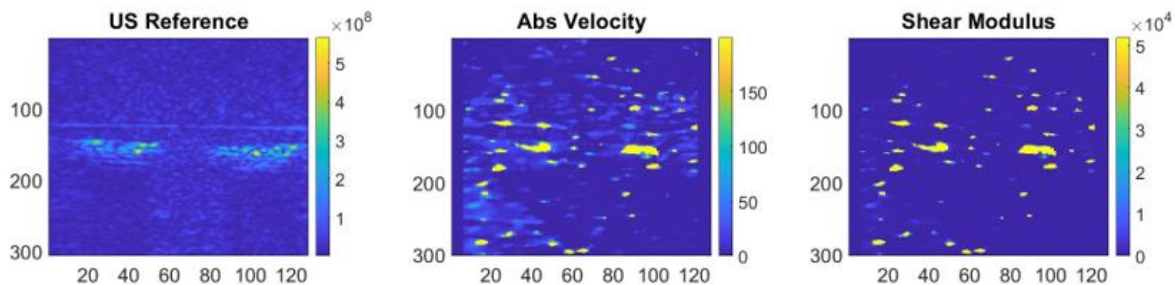


Figure 9: SWE Nondegraded BPLP-AT 5%, 10% Right Side Filtered

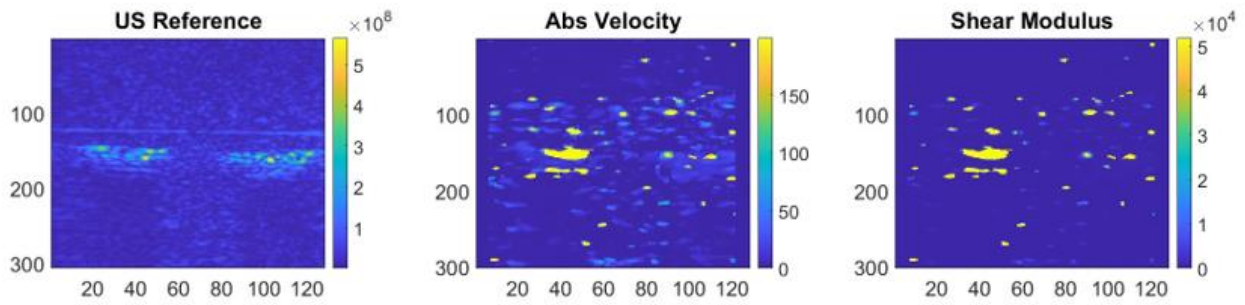


Figure 10: SWE Nondegraded BPLP-AT 5%, 10% Left Side Filtered

Figures 11 and 12 show the US reference, the absolute velocity of the shear wave propagated, and the shear modulus of the material of the nondegraded POC-FA 5% sample and POC-FA 10% sample respectively. It is seen by comparing the left side of the shear modulus contour plot in Figure 11 (POC-FA 5%) to the right side of the shear modulus contour plot in Figure 12 (POC-FA 10%) that an increase in the percent of FA added to POC leads to an increase in the material's shear modulus. This is seen by a more intense marking in the locations of each material as seen in the respective US reference images.

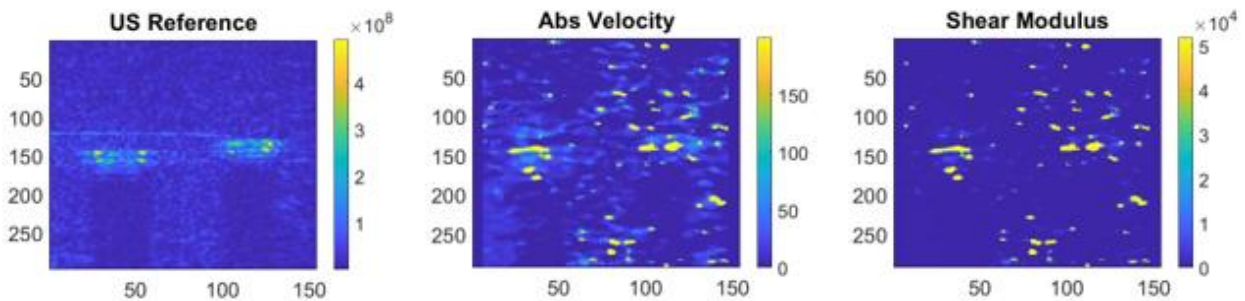


Figure 11: SWE Nondegraded POC-FA 5%, 10% Right Side Filtered

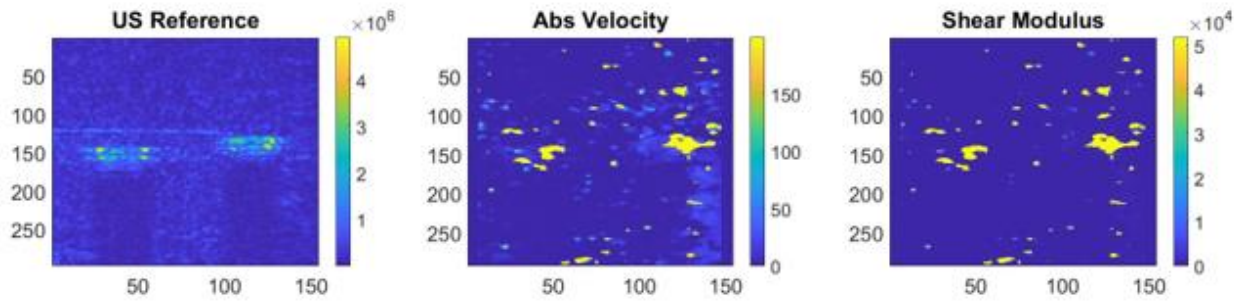


Figure 12: SWE Nondegraded POC-FA 5%, 10% Left Side Filtered

Figures 13 and 14 show the US reference, the absolute velocity of the shear wave propagated, and the shear modulus of the material of the one hour degraded BPLP-AT 5% sample and BPLP-AT 10% sample respectively. Similar to the nondegraded BPLP-AT samples, it is seen that in one hour degraded samples, an increase in the percent of AT added to BPLP leads to decrease in the material's shear modulus.

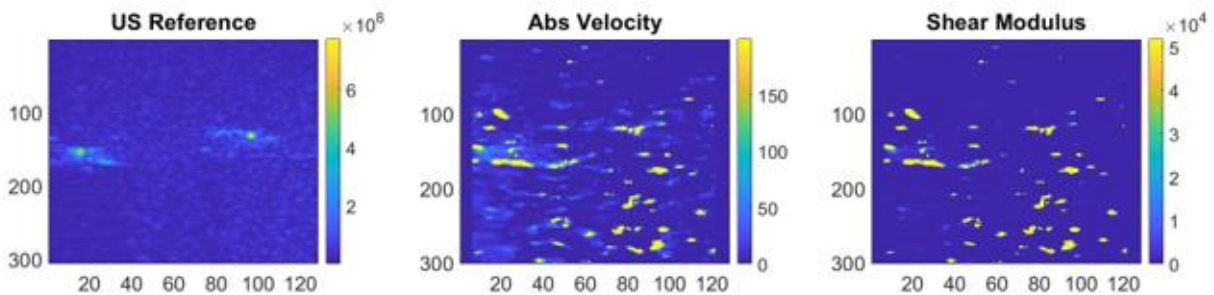


Figure 13: SWE 1 Hour Degraded BPLP-AT 5%, 10% Right Side Filtered

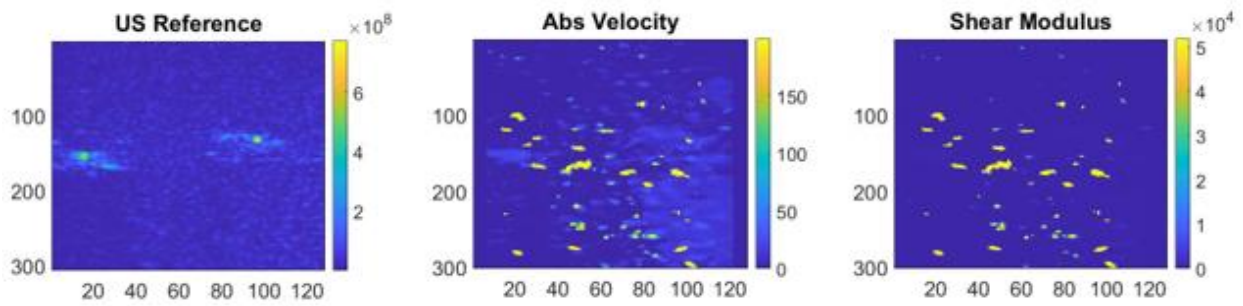


Figure 14: SWE 1 Hour Degraded BPLP-AT 5%, 10% Left Side Filtered

Figures 15 and 16 show the US reference, the absolute velocity of the shear wave propagated, and the shear modulus of the material of the one hour degraded POC-FA 5% sample and POC-FA 10% sample respectively. Similar to the nondegraded POC-FA samples, it is seen that in one hour degraded samples, an increase in the percent of FA added to POC leads to an increase in the material's shear modulus.

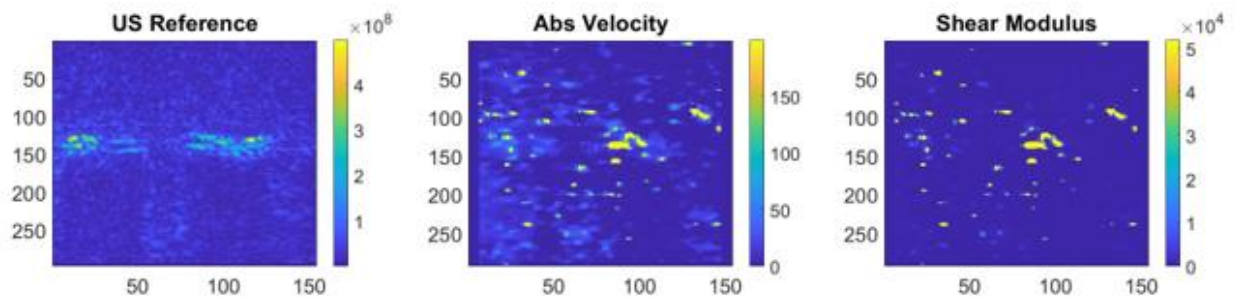


Figure 15: SWE 1 Hour Degraded POC-FA 5%, 10% Right Side Filtered

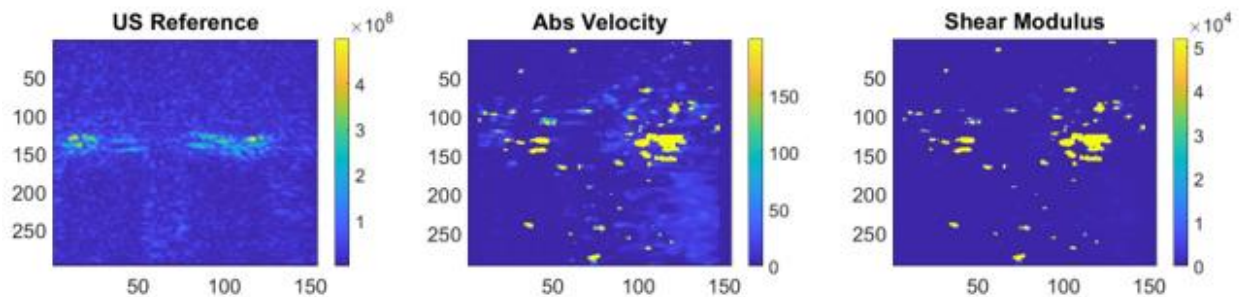


Figure 16: SWE 1 Hour Degraded POC-FA 5%, 10% Left Side Filtered

Figures 17 and 18 show the US reference, the absolute velocity of the shear wave propagated, and the shear modulus of the material of the two hours degraded BPLP-AT 5% sample and BPLP-AT 10% sample respectively. Like the nondegraded and one hour degraded BPLP-AT samples, it is seen that in two hour degraded samples, an increase in the percent of AT added to BPLP leads to a decrease in the material's shear modulus.

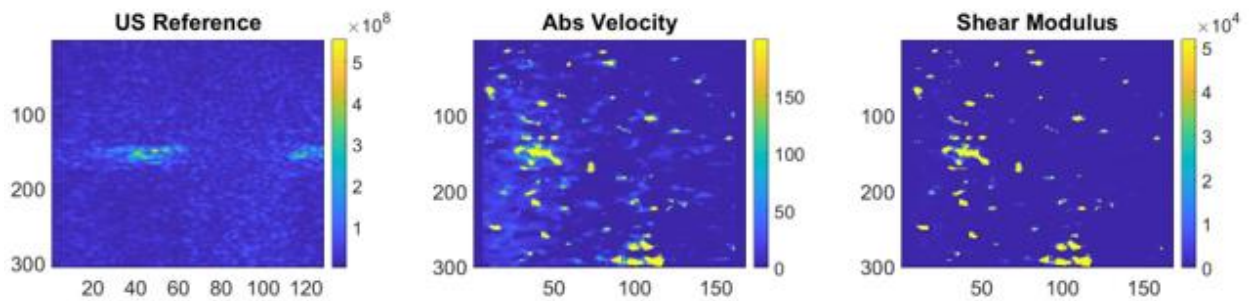


Figure 17: SWE 2 Hours Degraded BPLP-AT 5%, 10% Right Side Filtered

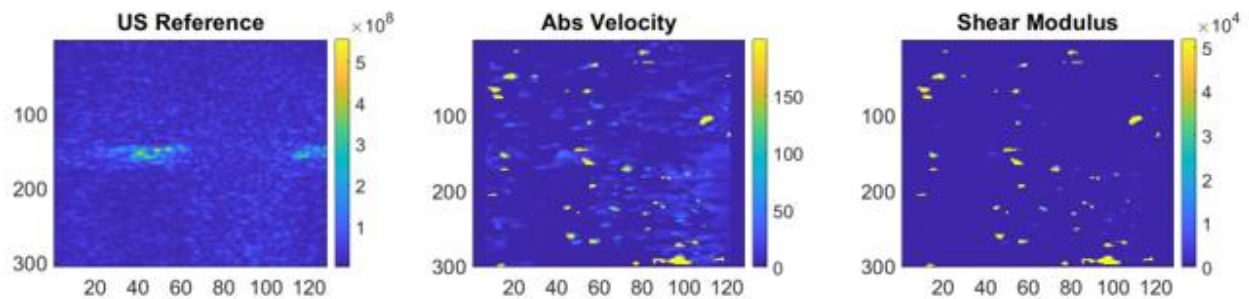


Figure 18: SWE 2 Hours Degraded BPLP-AT 5%, 10% Left Side Filtered

Figures 19 and 20 show the US reference, the absolute velocity of the shear wave propagated, and the shear modulus of the material of the two hours degraded POC-FA 5% sample and POC-FA 10% sample respectively. Like the nondegraded and one hour degraded POC-FA samples, it is seen that in two hour degraded samples, an increase in the percent of FA added to POC leads to an increase in the material's shear modulus.

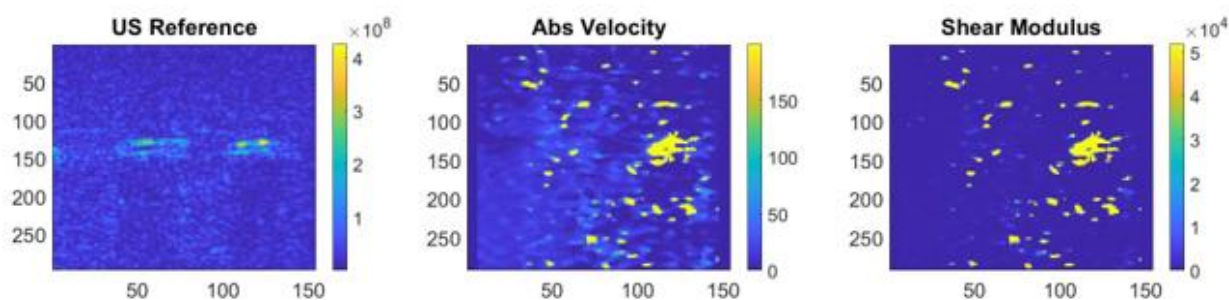


Figure 19: SWE 2 Hours Degraded POC-FA 5%, 10% Right Side Filtered

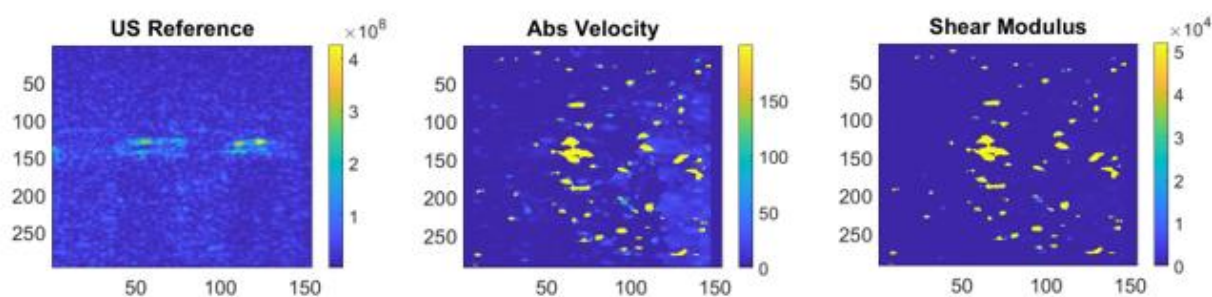


Figure 20: SWE 2 Hours Degraded POC-FA 5%, 10% Left Side Filtered

Figures 21 and 22 show the US reference, the absolute velocity of the shear wave propagated, and the shear modulus of the material of the four hours degraded BPLP-AT 5% sample and BPLP-AT 10% sample respectively. As previous BPLP-AT samples showed, four hour degraded samples likewise showed that an increase in the percent of AT added to BPLP leads to a decrease in the material's shear modulus.

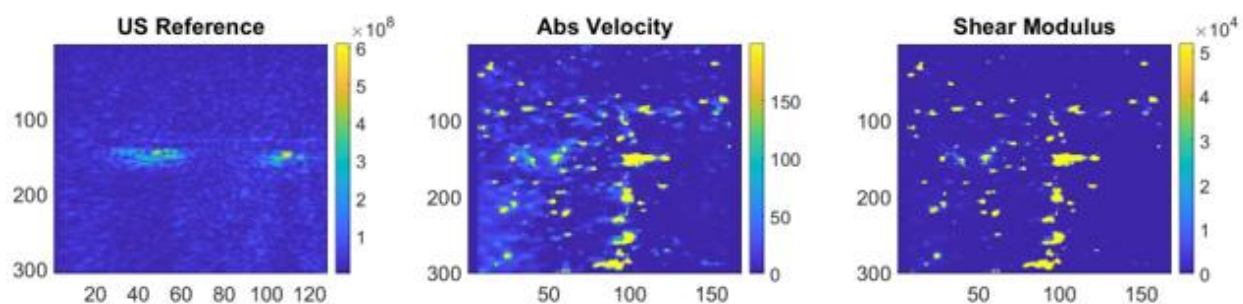


Figure 21: SWE 4 Hours Degraded BPLP-AT 5%, 10% Right Side Filtered

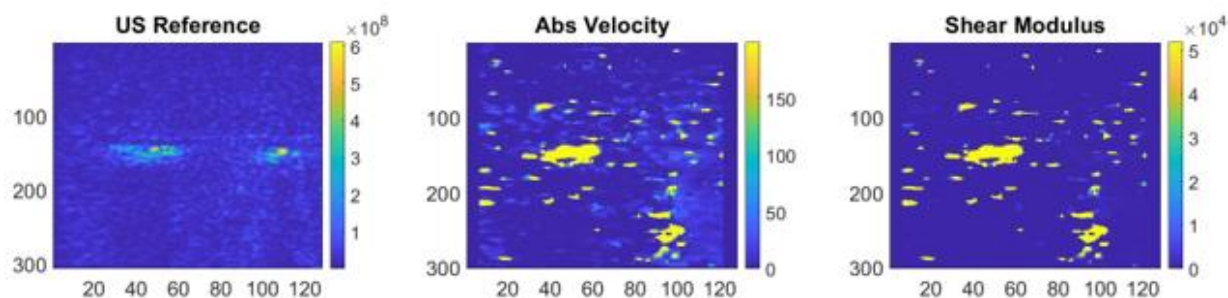


Figure 22: SWE 4 Hours Degraded BPLP-AT 5%, 10% Left Side Filtered

Figures 23 and 24 show the US reference, the absolute velocity of the shear wave propagated, and the shear modulus of the material of the four hours degraded POC-FA 5% sample and POC-FA 10% sample respectively. As previous POC-FA samples showed, four hour degraded samples likewise showed that an increase in the percent of FA added to POC leads to an increase in the material's shear modulus.

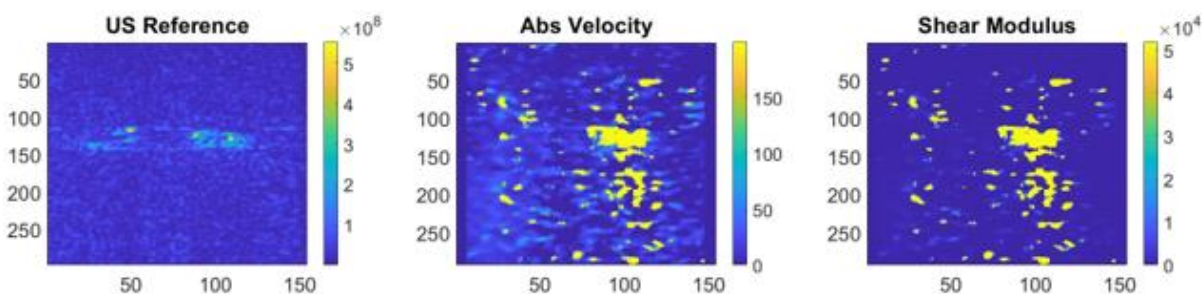


Figure 23: SWE 4 Hours Degraded POC-FA 5%, 10% Right Side Filtered

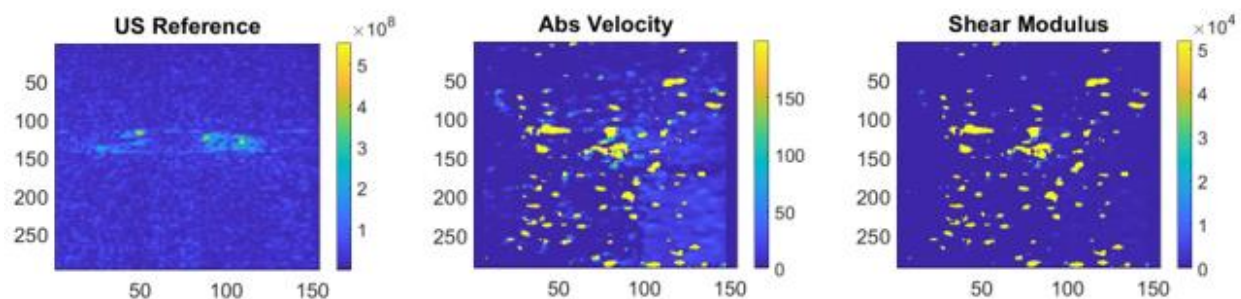


Figure 24: SWE 4 Hours Degraded POC-FA 5%, 10% Left Side Filtered

Figures 25 and 26 show the US reference, the absolute velocity of the shear wave propagated, and the shear modulus of the material of the continual degradation of BPLP-AT 5% at one, two, four eight and twelve hours. It is seen by comparing the left side of the shear modulus contour plot in Figure 25 (BPLP-AT 5% one hour degraded and two hours degraded) to the right side of the shear modulus contour plot in Figure 26 (BPLP-AT 5% four, eight and twelve hours degraded), that the longer the BLPL-AT 5% degrades, the smaller it's shear modulus gets. This is seen by less intense markings in the locations of each material as seen in the respective US reference images.

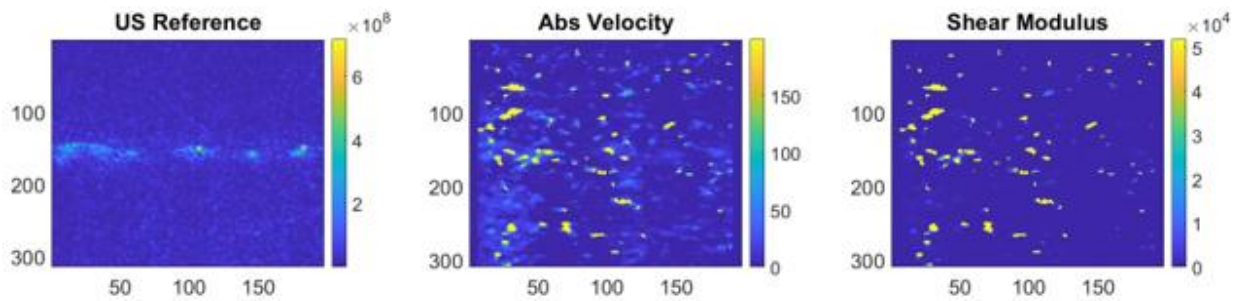


Figure 25: SWE 1, 2, 4, 8, 12 Hours Degraded BPLP-AT 5% Right Side Filtered

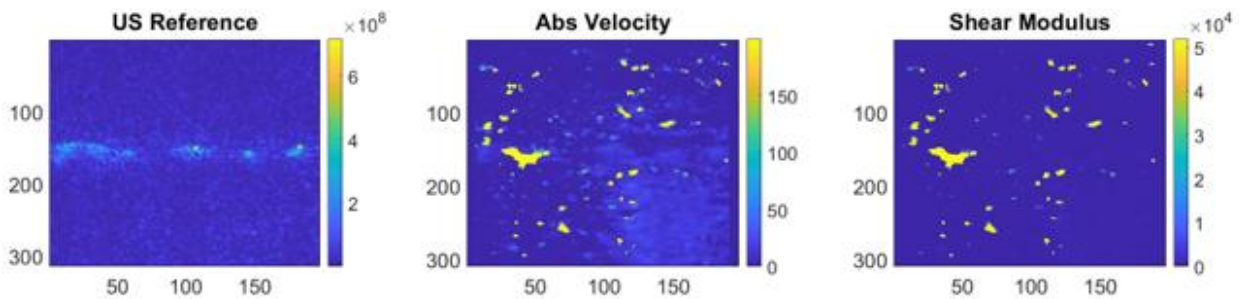


Figure 26: SWE 1, 2, 4, 8, 12 Hours Degraded BPLP-AT 5% Left Side Filtered

USPA Images

Below are the USPA images acquired from the five phantoms. The USPA images do not need a focus for wave propagation, nor do they require filtering. All the samples in each image are valid. Each USPA figure has three sub images. These images are the individual ultrasound and photoacoustic representations as well as the ultrasound and photoacoustic representations overlapped in one image. Figure 27 shows the locations of the various samples within the phantoms as well as the level at which the USPA images being viewed at.

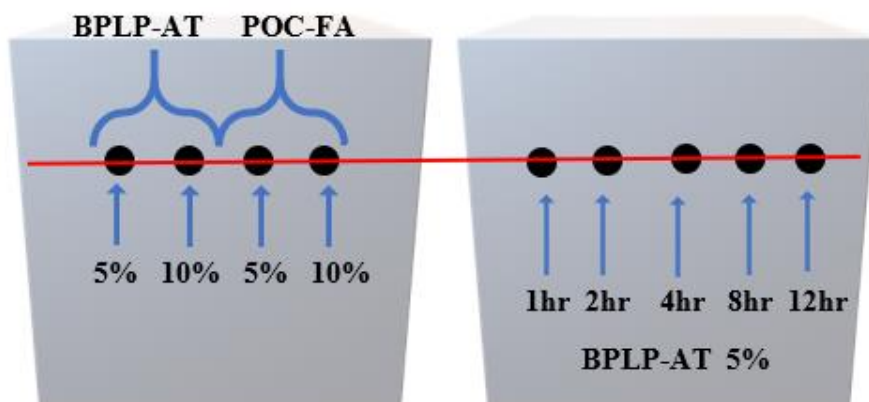


Figure 27: BPLP-AT 5%, 10% and POC-FA 5%, 10% Phantoms - All Levels of Degradation and BPLP-AT 5% Continual Degradation Phantom

In the USPA images, the middle, photoacoustic representation is the image of most interest. The ultrasound images show the location of the samples which is something that is able to be visualized with the naked eye. However, they are included for referencing. It should be noted that the brighter red the materials show in the photoacoustic images, the better their light absorbing properties are.

The photoacoustic image in Figure 28 shows the nondegraded samples for both percentages of each the BPLP-AT and POC-FA samples. It is seen that all four samples have satisfactory light absorbing properties. With an increase of BPLP-AT 5% to BPLP-AT 10% in the nondegraded samples, there is no

change in the light absorbing properties of BPLP-AT. However, with an increase of POC-FA 5% to POC-FA 10% in the nondegraded samples, there is an increase in light absorbing properties of POC-FA.

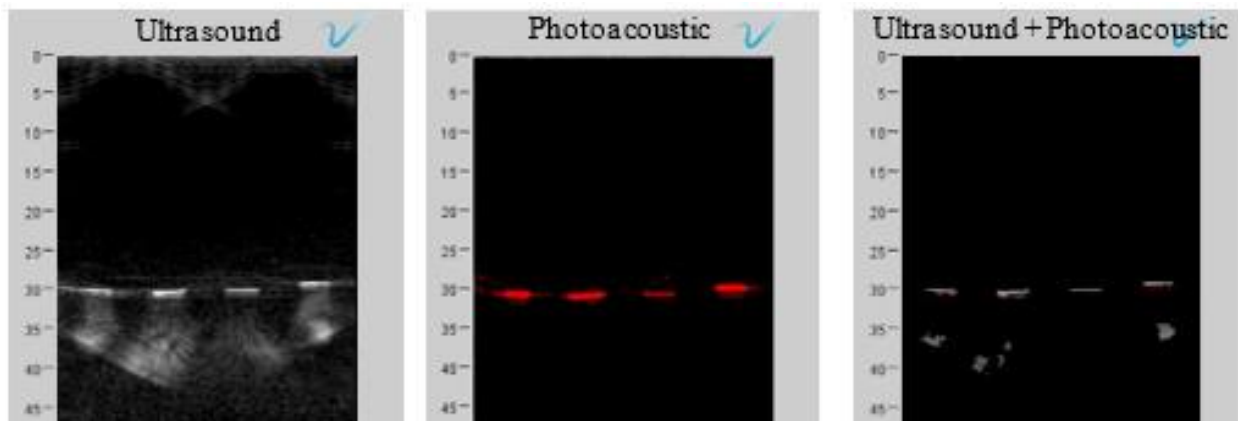


Figure 28: USPA Nondegraded BPLP-AT 5%, 10% and POC-FA 5%, 10%

The photoacoustic image in Figure 29 shows the one hour degraded samples for both percentages of each the BPLP-AT and POC-FA samples. Compared to the nondegraded samples, the one hour degraded samples have significantly worse light absorbing properties. With an increase of BPLP-AT 5% to BPLP-AT 10% in the one hour degraded samples, there is a decrease in the light absorbing properties of BPLP-AT. Like the nondegraded samples, with an increase of POC-FA 5% to POC-FA 10% in the one hour degraded samples, there is an increase in light absorbing properties of POC-FA.

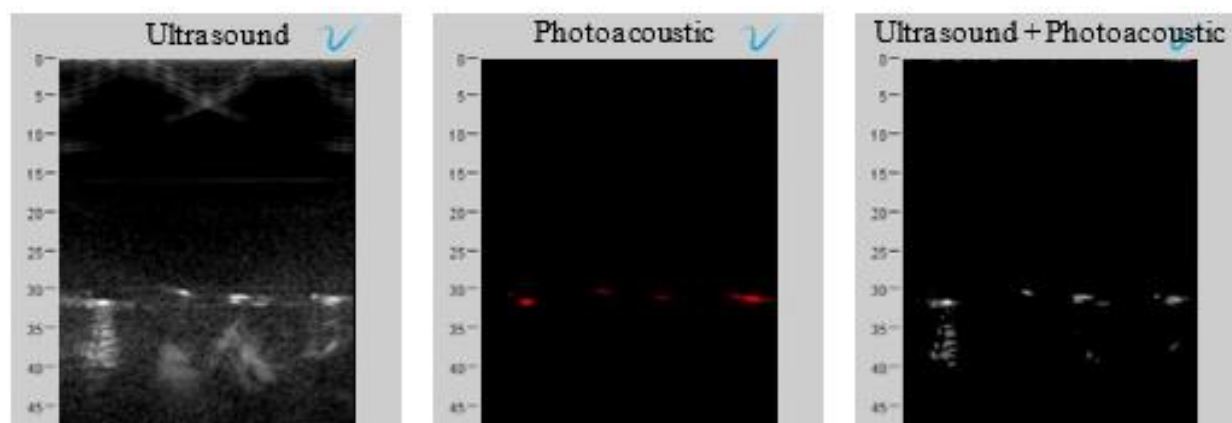


Figure 29: USPA 1 Hour Degraded BPLP-AT 5%, 10% and POC-FA 5%, 10%

The photoacoustic image in Figure 30 shows the two hour degraded samples for both percentages of each the BPLP-AT and POC-FA samples. As seen before, an increase of BPLP-AT 5% to BPLP-AT 10% leads to a decrease in the light absorbing properties of BPLP-AT. Similarly, an increase of POC-FA 5% to POC-FA 10% results in better light absorbing properties of POC-FA.

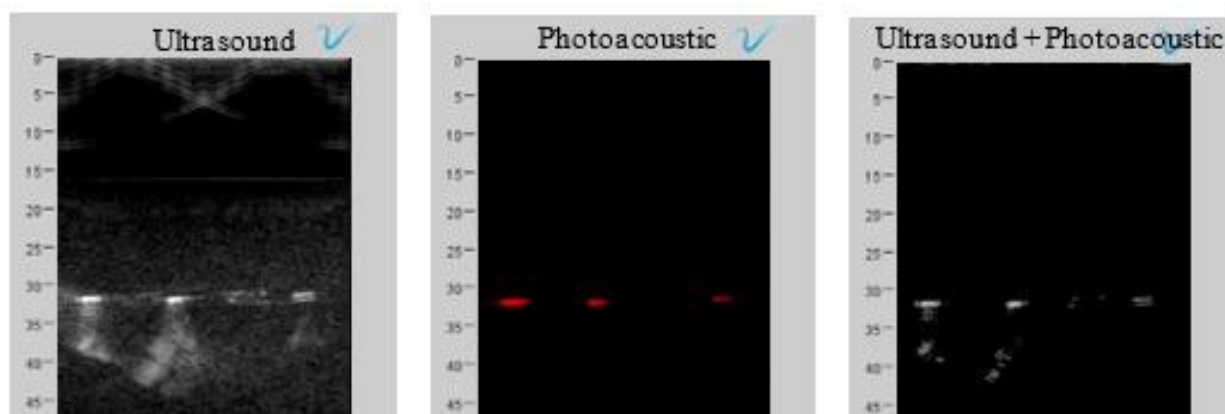


Figure 30: USPA 2 Hours Degraded BPLP-AT 5%, 10% and POC-FA 5%, 10%

The photoacoustic image in Figure 31 shows the four hour degraded samples for both percentages of each the BPLP-AT and POC-FA samples. By this point in the study, a correlation has begun to emerge.

An increase in the percent of AT in BPLP decreases the light absorbing properties while an increase in the percent of FA in POC increases the light absorbing properties.

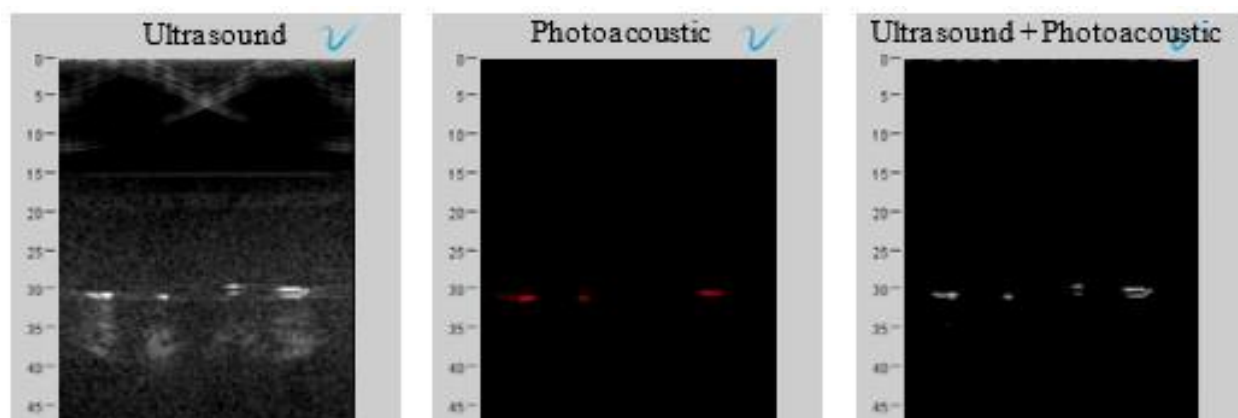


Figure 31: USPA 4 Hours Degraded BPLP-AT 5%, 10% and POC-FA 5%, 10%

The final set of USPA images, shown in Figure 32, compares the light absorbing properties of BPLP-AT 5% continually degraded over 1, 2, 4, 8, and 12 hours. It is easily seen that the longer the material degrades, the less light absorbing it is. This is likely because the samples lose size as they shrink but it could also be related to the material properties changing.

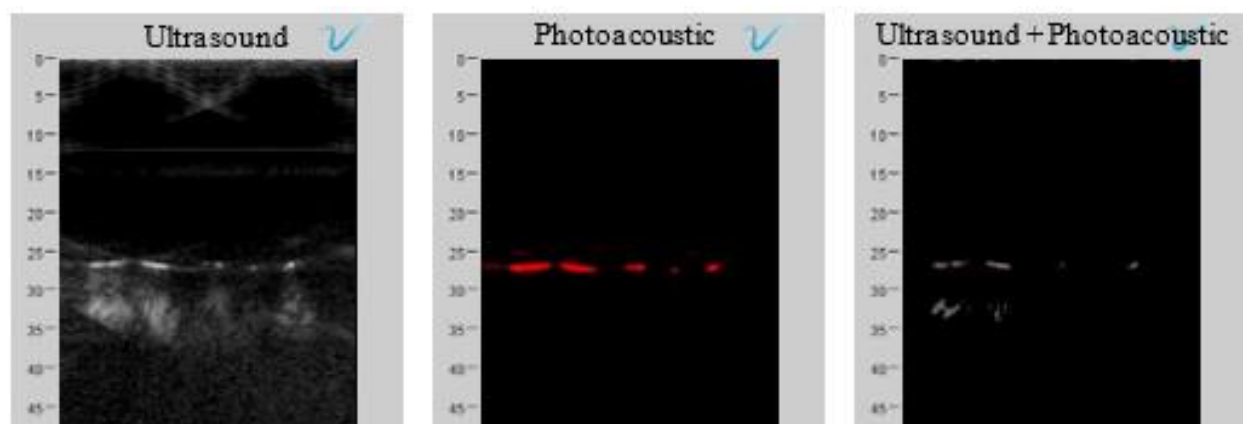


Figure 32: USPA 1, 2, 4, 8, 12 Hours Degraded BPLP-AT 5%

Chapter 5

Conclusion

BPLP-AT and POC-FA have varying material properties based on the percentage of AT and FA added respectively. From SWE imaging, conclusions about the material's shear modulus can be drawn. In each of the studies where BPLP-AT 5% and BPLP-AT 10% were not degraded and degraded for one, two and four hours, there was consistently a decrease the shear modulus of BPLP for a higher percent of AT. Contrarily, in each of the studies where POC-FA 5% and POC-FA 10% were not degraded and degraded for one, two and four hours, there was consistently an increase the shear modulus of POC for a higher percent of FA.

In addition to their material properties being dependent on the percentage of AT and FA added, BPLP-AT and POC-FA have varying material properties based on the time they are degraded for. Looking across the SWE images and comparing the same materials for increasing degradation times, it is seen for all BPLP-AT 5%, 10%, POC-FA 5%, 10% that an increase in degradation time leads to a decrease in shear modulus.

While information about the material's shear modulus can be drawn from SWE images, information about the material's light absorbing properties can be drawn from the USPA images. From all USPA images, it is seen that an increase in the percent of AT in BPLP decreases the light absorbing properties while an increase in the percent of FA in POC increases the light absorbing properties. Additionally, the longer the material degrades, the less light absorbing it is.

BIBLIOGRAPHY

- [1] “Peripheral Nerve Injury.” *Johns Hopkins Medicine*,
<https://www.hopkinsmedicine.org/health/conditions-and-diseases/peripheral-nerve-injury#:~:text=The%20peripheral%20nervous%20system%20is,and%20can%20be%20damaged%20easily.>
- [2] “Peripheral Nerve Injuries.” *Mayo Clinic*, Mayo Foundation for Medical Education and Research, 17 Apr. 2020, <https://www.mayoclinic.org/diseases-conditions/peripheral-nerve-injuries/symptoms-causes/syc-20355631>.
- [3] Vandergrindt, Carly. “Hereditary Neuropathy: Types, Risk Factors, Symptoms, and More.” *Healthline*, Healthline Media, 17 Sept. 2018, <https://www.healthline.com/health/hereditary-neuropathy>.
- [4] Boundless. “Boundless Anatomy and Physiology.” *Lumen*,
<https://courses.lumenlearning.com/boundless-ap/chapter/neurons/>.
- [5] “Myelin: Medlineplus Medical Encyclopedia.” *MedlinePlus*, U.S. National Library of Medicine,
<https://medlineplus.gov/ency/article/002261.htm#:~:text=Myelin%20is%20an%20insulating%20layer,efficiently%20along%20the%20nerve%20cells.>
- [6] Authors Christopher S. Ahuja, et al. “Why Doesn't Your Brain Heal like Your Skin?” *Frontiers for Young Minds*, <https://kids.frontiersin.org/articles/10.3389/frym.2016.00022>.
- [7] “Pinched Nerve.” *Mayo Clinic*, Mayo Foundation for Medical Education and Research, 22 Jan. 2022,
<https://www.mayoclinic.org/diseases-conditions/pinched-nerve/diagnosis-treatment/drc-20354751>.
- [8] Glynn, Patric. “Alternative Methods to Autologous Nerve Grafting for the Regeneration of the Peripheral Nervous System.” *Inquiries Journal*, Discussions, 1 Jan. 2007,
<http://www.inquiriesjournal.com/articles/840/alternative-methods-to-autologous-nerve-grafting->

- [17] “Citric Acid.” ScienceDaily, ScienceDaily,
https://www.sciencedaily.com/terms/citric_acid.htm#:~:text=In%20biochemistry%2C%20it%20is%20important,and%20acts%20as%20an%20antioxidant.
- [18] Shan, Dingying, et al. “Citrate-Based Fluorescent Biomaterials.” *Advanced Healthcare Materials*, vol. 7, no. 18, 2018, p. 1800532., <https://doi.org/10.1002/adhm.201800532>.
- [19] Zhu, Lei, et al. “Fabricating Poly(1,8-Octanediol Citrate) Elastomer Based Fibrous Mats via Electrospinning for Soft Tissue Engineering Scaffold.” *Journal of Materials Science: Materials in Medicine*, vol. 28, no. 6, 2017, <https://doi.org/10.1007/s10856-017-5906-7>.
- [20] Fernández-Villa, Daniel, et al. “Tissue Engineering Therapies Based on Folic Acid and Other Vitamin B Derivatives. Functional Mechanisms and Current Applications in Regenerative Medicine.” *International Journal of Molecular Sciences*, vol. 19, no. 12, 2018, p. 4068., <https://doi.org/10.3390/ijms19124068>.
- [21] Li, Qing, et al. “Elastomeric Polyurethane Porous Film Functionalized with Gastrodin for Peripheral Nerve Regeneration.” *Journal of Biomedical Materials Research Part A*, vol. 108, no. 8, 2020, pp. 1713–1725., <https://doi.org/10.1002/jbm.a.36937>.
- [22] Sahar, MuhammadSana Ullah, et al. “Bridging Larger Gaps in Peripheral Nerves Using Neural Prosthetics and Physical Therapeutic Agents.” *Neural Regeneration Research*, vol. 14, no. 7, 2019, p. 1109., <https://doi.org/10.4103/1673-5374.251186>.
- [23] Bikis, Christos, et al. “Three-Dimensional and Non-Destructive Characterization of Nerves inside Conduits Using Laboratory-Based Micro Computed Tomography.” *Journal of Neuroscience Methods*, vol. 294, 2018, pp. 59–66., <https://doi.org/10.1016/j.jneumeth.2017.11.005>.
- [24] Yusufu, Aihemaitijiang, et al. “Application of Custom Anatomy-Based Nerve Conduits on Rabbit Sciatic Nerve Defects: In Vitro and in Vivo Evaluations.” *Neural Regeneration Research*, vol. 14, no. 12, 2019, p. 2173., <https://doi.org/10.4103/1673-5374.262601>.

- [25] Liao, Chengde, et al. "Tissue-Engineered Conduit Promotes Sciatic Nerve Regeneration Following Radiation-Induced Injury as Monitored by Magnetic Resonance Imaging." *Magnetic Resonance Imaging*, vol. 34, no. 4, 2016, pp. 515–523., <https://doi.org/10.1016/j.mri.2015.12.004>.
- [26] 05, Mayfair • May. "How Does an Ultrasound Work?" *How Does an Ultrasound Work? | Mayfair Diagnostics*, <https://www.radiology.ca/article/how-does-ultrasound-work#:~:text=Also%20known%20as%20sonography%2C%20ultrasound,or%20soft%20tissue%20and%20bone>.
- [27] "How Do Ultrasound Examinations Work?" *Informedhealth.org*, <https://www.informedhealth.org/how-do-ultrasound-examinations-work.html>.
- [28] "Photoacoustic Imaging." *NanoHybrids*, <https://nanohybrids.net/pages/photoacoustic-imaging#:~:text=Photoacoustic%20imaging%20works%20by%20using,a%20pressure%20or%20acoustic%20wave>.
- [29] Beard, Paul. "Biomedical Photoacoustic Imaging." *Interface Focus*, vol. 1, no. 4, 2011, pp. 602–631., <https://doi.org/10.1098/rsfs.2011.0028>.
- [30] "What Is Photoacoustic Imaging?" *What Is Photoacoustic Imaging | FUJIFILM VisualSonics*, <https://www.visualsonics.com/photoacoustics-pa>.
- [31] An, Lu, and Benjamin T. Cox. "Estimating Relative Chromophore Concentrations from Multiwavelength Photoacoustic Images Using Independent Component Analysis." *Journal of Biomedical Optics*, vol. 23, no. 07, 2018, p. 1., <https://doi.org/10.1117/1.jbo.23.7.076007>.
- [32] Kawai, Tomonori. "Shear Wave Elastography for Chronic Musculoskeletal Problem." *Elastography - Applications in Clinical Medicine [Working Title]*, 2022, <https://doi.org/10.5772/intechopen.102024>.

ACADEMIC VITA

EDUCATION

- 2022 Bachelor of Science, Major: Biomedical Engineering, Minor: Engineering Mechanics
Pennsylvania State University State College, PA *Schreyer Scholar*
- 2018 Lakeview High School Stoneboro, PA

PROFESSIONAL EXPERIENCES

- 2020-22 Intern: employed through Bionic Pets, Sterling, VA
- Independently casted, molded, and fabricated custom braces and prostheses for pets
 - Set up an additive manufacturing station for braces
 - Used 3D scanning software for designing body jackets
 - Interacted with suppliers, customers, and patients
 - Works remotely during the school year: contacts customers for feedback on services; writes weekly newsletters highlighting recent cases and updates.
- 2019 Student Researcher (summer): Employed through Penn State University. Tensile tested and documented carbon nanocomposites. Utilized MATLAB to compute the numeric mechanical properties of the composite. Interpreted the data to draw conclusions and summarized the findings for presentation to professors and peers.

AWARDS

- Dean's list: 1st semester-present
- Accepted to present and publish Effect of Strain Rate on Tensile Properties of Injection Molded Multiwall Carbon Nanotube Reinforced PA 6/6 Nanocomposite at the International Mechanical Engineering Congress and Exposition
- Publication of Neurophysiology: Environmental Factors Affecting Neuron Function in the *2017 Journal of the Pennsylvania Governor's School for the Sciences*.
- Girl Scout Gold Award
- PSU Academic Excellence Scholarship, Chancellor's Scholarship-Behrend, Commonwealth Campus First Year Award Erie, Triangle STEAM Scholarship

VOLUNTEER EXPERIENCE

- 2020 Borrowed 3D printers from local high school, independently printed, assembled, and distributed over 800 face shields for frontline workers during the COVID pandemic.
- 2020 Student volunteer at the Penn State Arboretum, State College, PA

CLUBS AND ACTIVITIES

- 2018-20 Penn State Behrend Cross Country and Track and Field
- 2021-22 Penn State Club Cross Country